PHYSICAL REVIEW D VOLUME 50, NUMBER 5 1 SEPTEMBER 1994

Goldstone pion and other mesons using a scalar confining interaction

Franz Gross
Physics Department, College of William and Mary, Williamsburg, Virginia 23185
and Continuous Electron Beam Accelerator Facility, 12000 Jefferson Avenue, Newport News, Virginia 23606

Joseph Milana
Department of Physics and Center for Theoretical Physics, University of Maryland, College Park, Maryland 20742
(Received 28 February 1994)

A covariant wave equation for $q\bar{q}$ interactions with an interaction kernel composed of the sum of *constant vector* and *linear scalar* confining interactions is solved for states with two quarks with identical mass. The model includes a Nambu–Jona-Lasinio–like mechanism which links the dynamical breaking of chiral symmetry to the spontaneous generation of quark mass and the appearance of a low mass Goldstone pion. A novel feature of this approach is that it automatically explains the small mass of the pion *even though the linear potential is a scalar interaction in Dirac space, and hence breaks chiral symmetry.* Solutions for mesons composed of light quarks (π, ρ, and low lying excited states) and heavy quarks (η_c, J/Ψ, and low lying excited states) are presented and discussed.

PACS number(s): 12.39.−x, 11.10.St, 11.30.Rd, 14.40.−n

I. INTRODUCTION

In two previous papers [1,2] we have presented a covariant Nambu–Jona-Lasinio–like [3] model which is manifestly covariant and which includes confinment [4]. The quark-antiquark ($q\bar{q}$) interaction is a relativistic generalization of a potential consisting of a constant plus a linear confining term, and has two functions: (i) it dynamically generates quark mass through a Dyson equation for the quark self-energy, and (ii) it binds $q\bar{q}$ pairs into mesons (and can be extended to include the description of baryons as three quark states, but this extension has not yet been developed). As in the original Nambu–Jona-Lasinio (NJL) model (which, however, does *not* include confinement), our model guarantees that the dynamical generation of quark mass in the limit when the "bare," or undressed, quark mass is exactly zero (which we will refer to as the chiral limit) must be accompanied by the existence of a pseudoscalar bound state of zero mass (the pion). This occurs because the Dyson equation for the dynamical generation of quark mass and the equation for a pseudoscalar bound state of zero mass are identical in the limit when the current quark mass is zero, and hence the existence of a solution for one implies a solution for the other. In our previous papers we described in considerable detail how the relativistic confining interaction is defined, and how the relativistic equations are constructed in the general case. The equations are covariant, two-body equations with two channels: one with the *quark* restricted to its *positive* energy mass shell, and one with the *antiquark* restricted to its *negative* energy mass shell. The equations and model will be reviewed as needed below, but for an introductory discussion of all of these ideas the reader is referred to Refs. [1, 2].

In our original work, we assumed that the entire Dirac structure of the relativistic kernel which described the $q\bar{q}$ interaction was invariant under transformations of the chiral U(1) group. Later, in Ref. [2] we realized that, because of the constraint given in Eq. (1.3) below, it was not necessary for the purely linear part of the confining interaction to be chirally invariant, permitting us to use this model to explain the small mass of the pion *even when the linear potential is a scalar interaction in Dirac space, and hence breaks chiral symmetry.* It is the purpose of this paper to explore this attractive possibility further. As part of this exploration, we present numerical solutions for the first few bound states of both light and heavy mesons, which encourage the belief that, after the addition of the one-gluon-exchange mechanism (not discussed here), this model will both (i) provide a natural explanation of how the mass of the pion approaches zero in the chiral limit, and (ii) explain the entire spectrum of the "normal" mesons. A detailed discussion of the entire meson spectrum is postponed until the one-gluon-exchange mechanism has been added to the model.

In the rest of this section we will briefly describe the new model we are proposing. In Sec. II we discuss the dynamical generation of quark mass and in Sec. III present the exact form of the bound-state equations and wave functions for pseudoscalar and vector meson states. In Sec. IV, we discuss a family of pionlike solutions (including the physical pion state) and in Sec. V present solutions for the other "normal" mesons. Section VI presents our conclusions and includes a discussion of the relation of this work to other recent work, and some details are given in the Appendix.

In this paper the kernel which describes the interaction of a quark q with momentum $p_1 = p + \frac{1}{2}P$ and an antiquark $\bar{q}$ with momentum $p_2 = p - \frac{1}{2}P$, as illustrated in Fig. 1, is written in the form

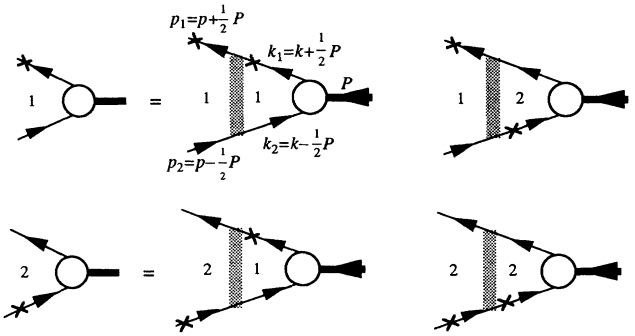

FIG. 1. Diagrammatic representation of the coupled channel bound state equations with the momenta and channel numbers labeled. The particle which is on shell is marked with an $\times$, and for channel 1 it is the quark and for channel 2 the antiquark. The wide shaded line connecting the two quarks represents the interaction kernel, which is a sum of constant plus linear terms.

$$\mathcal{V}(p,k)=\mathbf{F}_1\cdot\mathbf{F}_2\frac{3}{4}\left\{(2\pi)^3\,\delta(\mathbf{p}-\mathbf{k})\,\frac{E_p}{m}\,C\,\gamma_1^\mu\gamma_{2\mu}\right.$$
$$\left.+V_L(p,k)\mathbf{1}_1\mathbf{1}_2\right\}, \tag{1.1}$$

where m is the mass of the on-shell quark (or antiquark), $E_p=\sqrt{m^2+p^2}$, C is a constant, γ^μ are the Dirac γ matrices, and $\mathbf{F}_a=\frac{1}{2}\lambda_a$ are the SU(3) color matrices. The kernels $\mathcal{V}$ and V_L are functions of the relative four momenta (p and k) with energy components which depend on which quark is on shell, as discussed in Eq. (3.3). Note that both the relative four momentum and the *magnitude* of the relative three momentum will be denoted by p; the distinction should be clear from the context. The subscripts 1 and 2 on the Dirac matrices γ^μ and on the 4×4 unit matrix $\mathbf{1}$ label the particle on which the matrices act. On color singlet states, with the color flowing in the directions labeled in Fig. 1 the color operator $\mathbf{F}_1\cdot\mathbf{F}_2$ has the value

$$\mathbf{F}_1\cdot\mathbf{F}_2=\frac{4}{3}. \tag{1.2}$$

The function $V_L(p,k)$ is the momentum space representation for the linear, confining potential and is discussed in detail in Section III. For now it is sufficient to note that it satisfies the constraint

$$\int\frac{d^3k}{E_k}V_L(p,k)=0. \tag{1.3}$$

Using the specific form of V_L given in Sec. III, and taking the limit $m\to\infty$, the kernel (1.1) can be understood to be a relativistic, momentum space generalization of a coordinate space potential of the form

$$\mathcal{V}(r)=-C+\sigma r. \tag{1.4}$$

The change of sign in the constant term can be traced to the fact that the vector and scalar matrix elements for the antiquark have opposite sign:

$$\bar v(-\mathbf{p}_2)\,v(-\mathbf{p}_2)=-1,\quad \bar v(-\mathbf{p}_2)\,\gamma^0\,v(-\mathbf{p}_2)=\frac{E_p}{m}\to1 \tag{1.5}$$

and the fact that the effective sign of the interaction is determined by the sign of the scalar matrix elements.

The specific model (1.1) has many features already common to the models previously discussed in [1,2]. One new feature is that the linear and constant parts have a different Dirac structure. The linear part is a pure Dirac scalar, as suggested by lattice gauge calculations [5] and previous phenomenological fits to the meson spectrum [6]. The constant part is a pure vector, and is chirally invariant. Note also that both terms are multiplied by the color operator $\mathbf{F}_1\cdot\mathbf{F}_2$ and hence only colorless $q\bar q$ states will be confined [6].

II. DYNAMICAL GENERATION OF QUARK MASS

Quark mass is dynamically generated by the interaction given in Eq. (1.1). The equation for the quark self-energy predicted by this interaction can be obtained by starting with the four-dimensional Dyson equation:

$$\Sigma(p)=-i\int\frac{d^4k}{(2\pi)^4}\left\{\gamma^\mu\left[\frac{V_C(p,k)}{m_0-\not p+\Sigma(k)-i\epsilon}\right]\gamma_\mu\right.$$
$$\left.+\left[\frac{V_L(p,k)}{m_0-\not p+\Sigma(k)-i\epsilon}\right]\right\}, \tag{2.1}$$

where $V_C(p,k)$ is the (undefined) four-dimensional analog of $(2\pi)^3\,\delta(\mathbf{p}-\mathbf{k})\,\frac{E_p}{m}\,C$, and m_0 is the current quark mass, equal to zero in the chiral limit. Note that the color factor has been eliminated using (1.2).

Using the general form of the self-energy,

$$\Sigma(p)=\not p\,\Sigma_V(p^2)+\Sigma_S(p^2), \tag{2.2}$$

Eq. (2.1) can be reduced to

$$\frac{\Sigma(p)}{1-\Sigma_V(p^2)}=-i\int\frac{d^4k}{(2\pi)^4}\left\{\frac{V_C(p,k)[4m(k^2)-2\not k]-V_L(p,k)[m(k^2)+\not k]}{[1-\Sigma_V(p^2)]\,[1-\Sigma_V(k^2)]\,[m(k)^2-k^2-i\epsilon]}\right\}, \tag{2.3}$$

where the effective mass is

$$m(k^2) = \frac{m_0 + \Sigma_S(k^2)}{1 - \Sigma_V(k^2)}. \tag{2.4}$$

Our equation for the self-energy with the on-shell quark (or antiquark) constraint is obtained from (2.3) by integrating over dk_0 and retaining only the contribution from the positive energy quark pole. In this case $k^2 = m^2$, and the quantities $\Sigma_V = \Sigma_V^0$ and Σ_S become constants. Renormalizing the constants C, σ, and the current quark mass m_0 by

$$C \to \frac{C}{(1-\Sigma_V^0)^2}, \quad \sigma \to \frac{\sigma}{(1-\Sigma_V^0)^2}, \quad m_{0R} = \frac{m_0}{1-\Sigma_V^0} \tag{2.5}$$

and setting $p^2 = m^2$ gives the following equations:

$$\frac{\Sigma_V^0}{1-\Sigma_V^0} = -\int \frac{d^3k}{(2\pi)^3 2m}[2V_C(p,k) - V_L(p,k)],$$

$$m - m_{0R} = m\int \frac{d^3k}{(2\pi)^3 2E_k}[4V_C(p,k) - V_L(p,k)], \tag{2.6}$$

where we used the identity

$$\int d^3k \; k\!\!\!/ = p\!\!\!/ \int d^3k \frac{k\cdot p}{p^2}. \tag{2.7}$$

The first of Eqs. (2.6) will enable us to evaluate the renormalization constant $\frac{1}{1-\Sigma_V^0}$. The second gives a relation between the dynamical mass m, the renormalized current quark mass m_{0R}, and the (renormalized) strength of the constant potential, C. Using the constraint (1.3), this equation becomes simply

$$C = \frac{1}{2}(m - m_{0R}) \tag{2.8}$$

showing that $C \to \frac{1}{2}m$ in the chiral limit. In Sec. IV, we will use this equation and the value of C which emerges from our fit to the pion state to estimate the current quark mass.

III. THE EXACT BOUND-STATE EQUATIONS

The coupled equations which describe a bound state of four-momentum P coupled to a quark q with momentum $p_1 = p + \frac{1}{2}P$ and an antiquark $\bar{q}$ with momentum $p_2 = p - \frac{1}{2}P$, as illustrated in Fig. 1, can be written in the following form:

$$[\mathbf{G}^{-1}(p) - \mathbf{C}(p)]\,\Psi(p,P)$$

$$= -\int \frac{d^3k}{(2\pi)^3}\frac{\mathbf{V}(p,k;P)}{(1+\tilde{p}^2)(1+\tilde{k}^2)}\Psi(k,P), \tag{3.1}$$

where $\tilde{p} = p/(E_p + m)$ (with $E_p = \sqrt{m^2+p^2}$), and $\mathbf{G}^{-1}(p)$ is the inverse of the two-body Green's function, $\mathbf{C}(p)$ is the constant part of the interaction, and $\mathbf{V}(p,k;P)$ is the kernel of the integral operator which describes the linear, confining part of the interaction. This kernel is obtained by taking the appropriate matrix elements of the kernel given in (1.1).

For both pseudoscalar and vector states the wave function vector $\Psi(p,P)$ can be constructed from the following four rest-frame matrix elements of the $q\bar{q}$ vertex function $\Gamma(p,P)$:

$$\begin{aligned}
\phi_{1a}(\mathbf{p}) &= -\mathcal{N}\frac{m}{E_p}\frac{\bar{u}(\mathbf{p}_1,\lambda_1)\Gamma(p^{(1)},P)v(-\mathbf{p}_2,\bar{\lambda}_2)}{2E_p - m_B},\\
\phi_{1b}(\mathbf{p}) &= \mathcal{N}\frac{m}{E_p}\frac{\bar{u}(\mathbf{p}_1,\lambda_1)\Gamma(p^{(1)},P)u(\mathbf{p}_2,\lambda_2)}{m_B},\\
\phi_{2a}(\mathbf{p}) &= -\mathcal{N}\frac{m}{E_p}\frac{\bar{v}(-\mathbf{p}_1,\bar{\lambda}_1)\Gamma(p^{(2)},P)u(\mathbf{p}_2,\lambda_2)}{2E_p + m_B},\\
\phi_{2b}(\mathbf{p}) &= -\mathcal{N}\frac{m}{E_p}\frac{\bar{u}(\mathbf{p}_1,\lambda_1)\Gamma(p^{(2)},P)u(\mathbf{p}_2,\lambda_2)}{m_B},
\end{aligned} \tag{3.2}$$

where $u(\mathbf{p},\lambda)$ and $v(\mathbf{p},\bar{\lambda})$ are quark spinors, $\mathcal{N}$ is a normalization constant, and m_B is the mass of the bound state. The matrix elements $\phi_{1a,b}$ are associated with channel 1, in which the quark is restricted to its positive energy mass shell, while $\phi_{2a,b}$ are associated with channel 2, in which the antiquark is restricted to its negative energy mass shell. The energy component of the relative four momentum, p, is restricted in each of these channels, and we denote the relative four momentum in channel 1 by $p^{(1)}$ and in channel 2 by $p^{(2)}$. In the center of mass (c.m.) system, these restricted relative momenta are

$$p^{(1)} = (E_p - \tfrac{1}{2}m_B, \mathbf{p}), \qquad p^{(2)} = (E_p + \tfrac{1}{2}m_B, \mathbf{p}). \tag{3.3}$$

The structure and dimensionality of the wave function vector Ψ, and of the matrix operators $\mathbf{G}^{-1}(p)$, $\mathbf{C}(p)$, and $\mathbf{V}(p,k;P)$, are different for pseudoscalar and vector states. For pseudoscalar states, the matrix elements in Eq. (3.2) can each be expressed in terms of a *single* scalar function of the magnitude of the relative three-momentum. The expansions are

$$\phi_{ia}(\mathbf{p}) = u^{(i)}(p)\,\langle|\rangle, \qquad \phi_{ib}(\mathbf{p}) = v^{(i)}(p)\,\langle|\sigma\cdot\hat{\mathbf{p}}|\rangle, \tag{3.4}$$

where $u^{(i)}$ are S-state wave functions, $v^{(i)}$ are P-state wave functions, $\hat{\mathbf{p}}$ is the unit vector in the direction of $\mathbf{p}$, and the matrix elements in the two-component spin space are $\langle|\rangle = \langle\lambda_1|\lambda_2\rangle$ and $\langle|\sigma\cdot\hat{\mathbf{p}}|\rangle = \langle\lambda_1|\sigma\cdot\hat{\mathbf{p}}|\lambda_2\rangle$. The wave function vector $\Psi(p,P)$ is then defined to be the four-component vector constructed from the u and v wave functions

$$\Psi(p,P) = \begin{bmatrix} u^{(1)}(p) \\ v^{(1)}(p) \\ v^{(2)}(p) \\ u^{(2)}(p) \end{bmatrix}. \tag{3.5}$$

For vector states, the matrix elements (3.2) require *two* scalar functions for their complete description:

$$\phi_{ia}(\mathbf{p}) = u^{(i)}(p)\,\langle|\sigma\cdot\xi|\rangle + w^{(i)}(p)\frac{1}{\sqrt{2}}\,\langle|\,[3\xi\cdot\hat{\mathbf{p}}\,\sigma\cdot\hat{\mathbf{p}}-\sigma\cdot\xi]\,|\rangle,$$

$$\phi_{ib}(\mathbf{p}) = v_s^{(i)}(p)\,\sqrt{3}\,\langle|\xi\cdot\hat{\mathbf{p}}|\rangle - v_t^{(i)}(p)\,\sqrt{\frac{3}{2}}\,\langle|\,[\sigma\cdot\xi\sigma\cdot\hat{\mathbf{p}}-\xi\cdot\hat{\mathbf{p}}]\,|\rangle, \qquad (3.6)$$

where ξ is the spin-one polarization vector of the state, $u^{(i)}$ and $w^{(i)}$ are S- and D-state wave functions (respectively), and $v_s^{(i)}$ and $v_t^{(i)}$ are singlet and triplet P-state wave functions. For vector states the wave function $\Psi(p,P)$ is therefore an eight dimensional vector:

$$\Psi(p,P) = \begin{bmatrix} u^{(1)}(p) \\ w^{(1)}(p) \\ v_s^{(1)}(p) \\ v_t^{(1)}(p) \\ v_s^{(2)}(p) \\ v_t^{(2)}(p) \\ u^{(2)}(p) \\ w^{(2)}(p) \end{bmatrix}. \qquad (3.7)$$

The operators $\mathbf{G}^{-1}(p)$, $\mathbf{C}(p)$, and $\mathbf{V}(p,k;P)$ which enter Eqs. (3.1) are therefore 4×4 matrices for pseudoscalar states and 8×8 matrices for vector states. The Green's function $\mathbf{G}^{-1}(p)$ can be written

$$\mathbf{G}^{-1}(p) = \begin{bmatrix} (2E_p - m_B)\mathbf{1} & & & \\ & -m_B\mathbf{1} & & \\ & & m_B\mathbf{1} & \\ & & & (2E_p + m_B)\mathbf{1} \end{bmatrix}, \qquad (3.8)$$

where $\mathbf{1}$ is unity for pseudoscalar states and the 2×2 unit matrix for vector states. Similarly, the "constant" part of the interaction can be written

$$\mathbf{C}(p) = C\begin{bmatrix} \left(\frac{m}{E_p}+\frac{2p^2}{mE_p}\right)\mathbf{1} & -\frac{p}{E_p}\mathbf{a} & -\frac{p}{E_p}\mathbf{a} & T\left(\frac{m}{E_p}\mathbf{1}+\frac{2p^2}{3mE_p}\mathbf{b}\right) \\ -\frac{p}{E_p}\mathbf{a}^T & \frac{m}{E_p}\mathbf{1} & \frac{m}{E_p}\mathbf{1} & -\frac{p}{E_p}\mathbf{c} \\ -\frac{p}{E_p}\mathbf{a}^T & \frac{m}{E_p}\mathbf{1} & \frac{m}{E_p}\mathbf{1} & -\frac{p}{E_p}\mathbf{c} \\ T\left(\frac{m}{E_p}\mathbf{1}+\frac{2p^2}{3mE_p}\mathbf{b}\right) & -\frac{p}{E_p}\mathbf{c} & -\frac{p}{E_p}\mathbf{c} & \left(\frac{m}{E_p}+\frac{2p^2}{mE_p}\right)\mathbf{1} \end{bmatrix}, \qquad (3.9)$$

where C is a constant, $\mathbf{1}$ was defined above, $T=-3(+1)$ for pseudoscalar (vector) states, and $\mathbf{a}$, $\mathbf{b}$, and $\mathbf{c}$ are all unity for pseudoscalar states and 2×2 matrices for the vector states:

$$\mathbf{a} = \frac{1}{\sqrt{3}}\begin{bmatrix} 1 & -\sqrt{2} \\ \sqrt{2} & 1 \end{bmatrix}, \qquad \mathbf{b} = \begin{bmatrix} 1 & \sqrt{2} \\ \sqrt{2} & 2 \end{bmatrix}, \qquad \mathbf{c} = \frac{1}{\sqrt{3}}\begin{bmatrix} 1 & \sqrt{2} \\ \sqrt{2} & -1 \end{bmatrix}. \qquad (3.10)$$

The linear, confining kernel can be written in the following block matrix form:

$$\mathbf{V}(p,k;P) = \begin{pmatrix} V_{11}\begin{bmatrix} \mathbf{A} & \mathbf{E}_+(p,k) \\ \mathbf{E}_+^T(k,p) & -\mathbf{D} \end{bmatrix} & V_{12}\begin{bmatrix} \mathbf{E}_+(p,k) & \mathbf{B} \\ -\mathbf{D} & \mathbf{E}_-^T(k,p) \end{bmatrix} \\ V_{21}\begin{bmatrix} \mathbf{E}_+^T(k,p) & -\mathbf{D} \\ \mathbf{B}^T & \mathbf{E}_-(p,k) \end{bmatrix} & V_{22}\begin{bmatrix} -\mathbf{D} & \mathbf{E}_-^T(k,p) \\ \mathbf{E}_-(p,k) & \mathbf{A} \end{bmatrix} \end{pmatrix}, \qquad (3.11)$$

where V_{ij} are the elementary kernels for the momentum space linear potentials (first worked out in Ref. [1] and given below); $\mathbf{A}$, $\mathbf{B}$, $\mathbf{D}$, and $\mathbf{E}$ are simple functions of p and k for pseudoscalars, and 2×2 matrix functions of p and k for vectors. For pseudoscalars [where $\mathbf{E}_\pm = \mathbf{E}_\pm(p,k)$]

$$\mathbf{A} = 1 - 2\tilde{p}\tilde{k}z + \tilde{p}^2\tilde{k}^2, \mathbf{B} = -\left(\tilde{p}^2+\tilde{k}^2+2\tilde{p}\tilde{k}z\right), \quad \mathbf{D} = z - 2\tilde{p}\tilde{k} + \tilde{p}^2\tilde{k}^2 z, \mathbf{E}_\pm = \tilde{k}\left(1-\tilde{p}^2\right) + \tilde{p}z(1-\tilde{k}^2). \qquad (3.12)$$

In these expressions, z is the cosine of the angle between $\hat{\mathbf{p}}$ and $\hat{\mathbf{k}}$. For vector states

$$\mathbf{A} = \begin{pmatrix} 1 - 2\tilde{p}\tilde{k}z + \tilde{p}^2\tilde{k}^2 - \frac{4}{3}\tilde{p}^2\tilde{k}^2(1-z^2) & -\frac{\sqrt{2}}{3}\tilde{p}^2\tilde{k}^2(1-z^2) \\ -\frac{\sqrt{2}}{3}\tilde{p}^2\tilde{k}^2(1-z^2) & P_2(z) - 2\tilde{p}\tilde{k}z + \tilde{p}^2\tilde{k}^2 \\ & -\frac{1}{6}\tilde{p}^2\tilde{k}^2(1-z^2) \end{pmatrix},$$

$$\mathbf{B} = \frac{1}{3}\begin{pmatrix} -(\tilde{p}^2 + \tilde{k}^2 + 2\tilde{p}\tilde{k}z) & 2\sqrt{2}\left(\tilde{p}^2 P_2(z) + \tilde{k}^2 + 2\tilde{p}\tilde{k}z\right) \\ 2\sqrt{2}\left(\tilde{k}^2 P_2(z) + \tilde{p}^2 + 2\tilde{p}\tilde{k}z\right) & (\tilde{k}^2 + \tilde{p}^2)P_2(z) + 2\tilde{p}\tilde{k}z \end{pmatrix},$$

$$\mathbf{D} = \begin{pmatrix} z(1 - 2\tilde{p}\tilde{k}z + \tilde{p}^2\tilde{k}^2) & 0 \\ 0 & z(1 - 2\tilde{p}\tilde{k}z + \tilde{p}^2\tilde{k}^2) - \tilde{p}\tilde{k}(1-z^2) \end{pmatrix},$$

$$\mathbf{E}_{\pm} = \frac{1}{\sqrt{3}}\begin{pmatrix} \tilde{k}\left(1-\tilde{p}^2\right) + \tilde{p}z(1-\tilde{k}^2) & \mp\sqrt{2}(\tilde{k} + \tilde{p}z)(1 - \tilde{p}\tilde{k}z) \\ +2\tilde{p}^2\tilde{k}(1-z^2) & \\ \sqrt{2}[\tilde{p}z(1 - 2\tilde{p}\tilde{k}z - \tilde{k}^2) & \pm[\tilde{p}z(1-\tilde{k}^2) - \tilde{p}^2\tilde{k}(1+z^2) \\ +\tilde{k}(1+\tilde{p}^2)P_2(z)] & +\tilde{k}(1+\tilde{p}^2)P_2(z)] \end{pmatrix}, \tag{3.13}$$

where $P_2(z) = (3z^2 - 1)/2$ is the Legendre polynomial of order 2.

Finally, the elementary kernels V_{ij}, which describe how the linear potential connects the two channels, can be obtained from the generic kernel in Eq. (1.1) by substituting the appropriate momenta

$$V_{ij}(p,k) = V_L(p^{(i)}, k^{(j)}) , \tag{3.14}$$

being careful to include the treatment of singularities appropriate to each combination of momenta. Explicitly,

$$V_{ii}(p,k) = V_A(p^{(i)}, k^{(i)}) - E_k\delta(\mathbf{p}-\mathbf{k})\int \frac{d^3k'}{E_{k'}} V_A(p^{(i)}, k'^{(i)}), \quad i = 1\,,2$$

$$V_{21}(p,k) = \begin{cases} V_A(p^{(2)}, k^{(1)}) - E_k\delta(\xi(p)k_-\hat{\mathbf{p}} - \mathbf{k})\displaystyle\int_{k'<k_-} \frac{d^3k'}{E_{k'}} V_A(p^{(2)}, k'^{(1)}) & \text{if } k < k_- \\ 0 \qquad\qquad\qquad\qquad\qquad\qquad\qquad\qquad\qquad\qquad & \text{if } k_- < k < k_+ \\ V_A(p^{(2)}, k^{(1)}) - E_k\delta(k_b\hat{\mathbf{p}} - \mathbf{k})\displaystyle\int_{k'>k_+} \frac{d^3k'}{E_{k'}} V_A(p^{(2)}, k'^{(1)}) & \text{if } k_+ < k \end{cases}$$

$$V_{12}(p,k) = \begin{cases} V_A(p^{(1)}, k^{(2)}) - E_p\delta(\xi(k)p_-\hat{\mathbf{k}} - \mathbf{p})\displaystyle\int_{p'<p_-} \frac{d^3p'}{E_{p'}} V_A(p'^{(1)}, k^{(2)}) & \text{if } p < p_- \\ 0 \qquad\qquad\qquad\qquad\qquad\qquad\qquad\qquad\qquad\qquad & \text{if } p_- < p < p_+ \\ V_A(p^{(1)}, k^{(2)}) - E_p\delta(p_+\hat{\mathbf{k}} - \mathbf{p})\displaystyle\int_{p'>p_+} \frac{d^3p'}{E_{p'}} V_A(p'^{(1)}, k^{(2)}) & \text{if } p_+ < p, \end{cases} \tag{3.15}$$

where the integration regions for V_{12} and V_{21} are bounded by

$$k_{\mp} = \left| p \mp \frac{m_B(2E_p + m_B)}{2(E_p \mp p + m_B)} \right| \tag{3.16}$$

(with $p \to k$ for the quantities $p_{\mp}$), and

$$\xi(p) = \begin{cases} 1 \quad \text{if } m_B < m \quad \text{and} \quad p > \frac{m_B}{2}\left[1 + \frac{m}{m-m_B}\right] \\ -1 \quad \text{otherwise}\,. \end{cases} \tag{3.17}$$

The function V_A can be written

$$V_A(p^{(i)}, k^{(j)}) = -8\pi\sigma\, f\left(p_1^2\right)\, f\left(p_2^2\right)\left[\frac{1}{q^4} - \frac{1}{\Lambda^4 + q^4}\right] \times f\left(k_1^2\right)\, f\left(k_2^2\right) \tag{3.18}$$

where Λ is cutoff mass, q^2 is the square of the momentum transferred by the quark, f is a quark form factor

$$f(p^2) = \left[\frac{(\Lambda_q^2 - m^2)^2}{(\Lambda_q^2 - m^2)^2 + (m^2 - p^2)^2}\right]^2 , \tag{3.19}$$

and the values of p_1, p_2, k_1, and k_2 depend on the choice of channel. For channel (1), the quark (with momentum p_1) is on shell, while for channel (2) the antiquark (with momentum p_2) is on shell. Hence, in the rest system of the bound state we have

$$\text{channel (1)} \Rightarrow \begin{cases} p_1^2 = m^2, \;\; p_2^2 = (p_1 - P)^2 = m^2 + m_B^2 - 2E_p m_B, \\ f(p_1^2) f(p_2^2) = f(m^2 + m_B^2 - 2E_p m_B), \end{cases} \tag{3.20}$$

$$\text{channel (2)} \Rightarrow \begin{cases} p_2^2 = m^2, \;\; p_1^2 = (p_2 + P)^2 = m^2 + m_B^2 + 2E_p m_B, \\ f(p_1^2) f(p_2^2) = f(m^2 + m_B^2 + 2E_p m_B) \, . \end{cases}$$

Similarily, while the momentum transferred by the quark is $q^2 = (p_1 - k_1)^2$, its specific form depends on the channel assignments:

$$\begin{aligned} &\text{for } V_{11} \text{ or } V_{22} \qquad q^2 = (E_p - E_k)^2 - (\mathbf{p} - \mathbf{k})^2, \\ &\text{for } V_{12} \qquad q^2 = (E_p - E_k - m_B)^2 - (\mathbf{p} - \mathbf{k})^2, \\ &\text{for } V_{21} \qquad q^2 = (E_p - E_k + m_B)^2 - (\mathbf{p} - \mathbf{k})^2 \, . \end{aligned} \tag{3.21}$$

The physics behind the construction of the V_{ij} was discussed in detail in Refs. [1, 2], so here we will only comment briefly on several features of the result.

(i) The potentials are Hermitian. This means that $V_{ij}(p,k) = V_{ji}(k,p)$. The diagonal elements are therefore symmetric under interchange of $\mathbf{p}$ and $\mathbf{k}$, while the off-diagonal elements map into each other under this interchange.

(ii) The singularties of the kernels are regularized by the constraints

$$\begin{aligned} &\int d^3k \frac{m}{E_k} V_{ij}(p,k) = 0, \qquad \text{for } i \geq j \\ &\int d^3p \frac{m}{E_p} V_{12}(p,k) = 0 \, . \end{aligned} \tag{3.22}$$

In the nonrelativistic limit (i.e., when $m \to \infty$) the constraints on the diagonal kernels reduce to

$$\int d^3k \, V(\mathbf{p} - \mathbf{k}) = \int d^3p \, V(\mathbf{p} - \mathbf{k}) = 0, \tag{3.23}$$

which is the momentum space form of the statement that a purely linear nonrelativistic potential $V(r) = \sigma r$ is zero at $r = 0$. The constraints on the off-diagonal kernels are extensions of those for the diagonal kernels, and are consistent with the Hermiticity requirement.

(iii) The quark form factors (discussed in Ref. [2]) are unity when the quark (or antiquark) is on shell, and hence there is always only one form factor for the initial and final state, as given in Eq. (3.20). When the bound-state mass $m_B = 0$, the mass of the off-shell quark approaches m and the form factors become unity. Introduction of quark form factors was found to be necessary [2] in order to ensure that integrals over the kernels approach zero as the external momenta approach infinity.

(iv) The off-diagonal kernels are equal to the diagonal ones when the bound state mass $m_B = 0$. This is a natural feature of the definitions and essential for recovery of the chiral limit. However, when m_B is large (in comparison with the mean internal momentum of the bound state), the kernel V_{11} is much larger than the off-diagonal kernels (because the effective q^2 transferred by the quark is then much larger in V_{12} and V_{21} than in V_{11}), and also much larger than the kernel V_{22} (because of the m_B dependence of the quark form factors).

This concludes our review of the full set of coupled equations implied by our model. In applications we will reduce these equations to a smaller set by making approximations appropriate to the sector under consideration. In practice there are two sectors of interest. In the first sector (the pion), the bound-state mass $m_B = \mu$ is small compared to the quark mass m, and also small compared to the mean internal momentum p_0 of the bound quarks. In this sector the off-diagonal kernels are nearly as large as the diagonal kernels, and cannot be neglected, but other approximations are possible. This sector is examined in Sec. IV. In the second sector (all other states considered in this paper), the bound-state mass m_B is comparable to twice the quark mass, and large compared to the mean internal momentum p_0 of the bound quarks. For these states we may safely neglect the coupling to the second channel. The validity of this approximation (which is excellent) was studied for the case of the (unrealistic) chiral confining interaction in Ref. [1]. This approximation will be used in Sec. V in our discussion of the light quark vector mesons (the excited pion and the ρ and its excited states) and the heavy quark states (the $c\bar{c}$ states).

IV. THE PION

In this section we discuss the solutions for the pion, which is the only meson which has a very small mass $m_B = \mu$. As discussed in Refs. [1, 2], the equations have been designed to give a natural explanation for the emergence of a zero mass Goldstone boson in the chiral limit, and our focus here is to show how this feature is preserved *even when the linear potential is a scalar, which breaks chiral symmetry.*

A. Solutions

In the limit when $\mu \to 0$, the coupled equations (3.1) reduce to only three independent equations,

$$2E_p\left(1-\frac{2C}{m}\right)u^{(-)}(p) = -\int \frac{d^3k}{(2\pi)^3}V_0(p,k)u^{(-)}(k),$$

$$\left(2E_p+2C\frac{m}{E_p}\right)u^{(+)}(p)+2C\frac{p}{E_p}v^{(+)}(p) = -\int \frac{d^3k}{(2\pi)^3}\frac{V_0(p,k)}{(1+\tilde{p}^2)(1+\tilde{k}^2)}$$
$$\times\left\{\left[(1-\tilde{p})(1-\tilde{k})-4\tilde{p}\tilde{k}z\right]u^{(+)}(k)+\left[\tilde{k}(1-\tilde{p}^2)+\tilde{p}z(1-\tilde{k}^2)\right]v^{(+)}(k)\right\},$$

$$C\frac{p}{E_p}u^{(+)}(p)-C\frac{m}{E}v^{(+)}(p) = -\int \frac{d^3k}{(2\pi)^3}\frac{V_0(p,k)}{(1+\tilde{p}^2)(1+\tilde{k}^2)}$$
$$\times\left\{\left[\tilde{k}(1-\tilde{p}^2)+\tilde{p}z(1-\tilde{k}^2)\right]u^{(+)}(k)-\left[z-2\tilde{p}\tilde{k}+\tilde{k}^2\tilde{p}^2z\right]v^{(+)}(k)\right\}, \tag{4.1}$$

where the (+) and (−) combinations are

$$u^{(\pm)}(p) = u^{(1)}(p) \pm u^{(2)}(p) \tag{4.2}$$

and

$$V_0(p,k) = -8\pi\sigma\left[\frac{1}{q^4}-\frac{1}{\Lambda^4+q^4}\right] \tag{4.3}$$

with q^2 given in Eq. (3.21) (all three definitions are identical when $\mu = 0$). Note that there is no equation for $v^{(-)}(p)$; it must be fixed by other considerations. The basic definitions (3.2) and (3.4) show that, if $v^{(1)}(p)$ and $v^{(2)}(p)$ are finite in the limit $\mu \to 0$, then $v^{(-)}(p) = 0$ in this limit. We are assured that the first of the Eqs. (4.1) has the nontrivial solution

$$u^{(-)}(p) = \frac{\mathcal{N}}{E_p} \tag{4.4}$$

because this form satisfies the constraint (3.22), ensuring that the RHS of the equation is zero, and in the chiral limit $C \to \frac{1}{2}m$, ensuring that the LHS is also zero. However, no such special conditions hold for the last two of the Eqs. (4.1), and we therefore conclude that they are only solved by the "trivial" solution $u^{(+)}(p) = v^{(+)}(p) = 0$. The pion wave function vector (3.5) therefore reduces, in the chiral limit, to

$$\Psi(p,0) = \frac{\mathcal{N}}{E_p}\begin{bmatrix}1\\0\\0\\-1\end{bmatrix}. \tag{4.5}$$

This discussion leads to the conclusion that the P states should also be very small for the physical pion. Initial attempts to obtain numerical solutions to the equation with all four channels lead to difficulties, which we believe are associated with the fact that the equations reduce to only three independent equations in the $\mu \to 0$ limit. Hence we decided to approximate the equations by setting the P states to zero, and to obtain numerical solutions only for the two large S-state channels. It was found that a light quark mass of $m = m_u = 325$ MeV gave a reasonable mass for both the pion and the ρ, and all of our light quark solutions use this mass. With this mass fixed, we solved the coupled two channel S-state equations for "pions" with three different masses: 139.7,

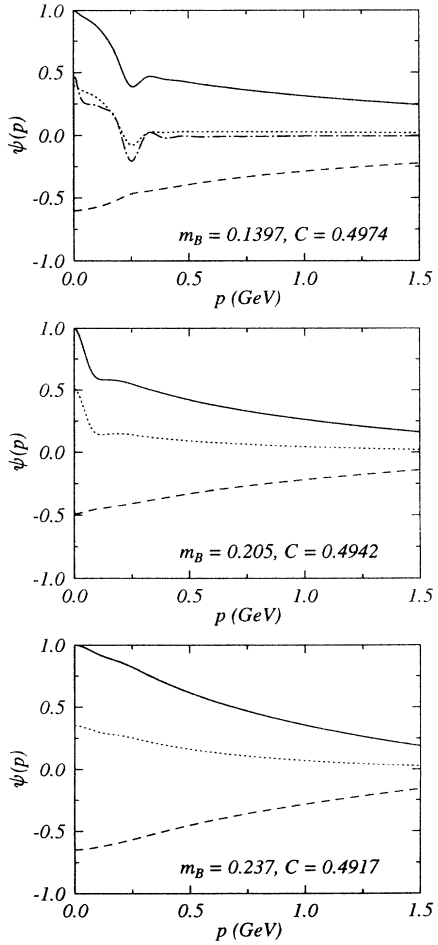

FIG. 2. Solutions for three pionlike states with masses m_B= 0.1397, 0.205, and 0.237 GeV. In each curve the solid line is $u^{(1)}$, the dashed line is $u^{(2)}$, and the dotted line is $u^{(1)}+u^{(2)}$. In the top figure, the dot-dash line is the integral Eq. (4.8), discussed in Sec. IV B.

TABLE I. Properties of the family of pionlike solutions discussed in the text. The quantities marked with an asterisk are obtained from the estimates given in Sec. IV B. The units of μ and p_0 are in GeV.

$\epsilon = 1 - 2\frac{C}{m_u}$	0.0052	0.0116	0.0166
μ	0.1397	0.205	0.237
μ^*	0.1396	0.207	0.249
p_0	1.26	0.84	0.73
p_0^*	1.26	0.84	0.71
f_+/f_-	0.059	0.120	0.142
$(f_+/f_-)^*$	0.076	0.131	0.159

205, and 237 MeV. The S-state wave functions for each of these pions is given in Fig. 2. Key properties of these solutions are summarized in Table I. This table gives the mass μ of each state, the values of the small parameter $\epsilon = 1 - 2\frac{C}{m_u}$ from which the "eigenvalue" C can be extracted, the mean momentum p_0 of each state, and the ratio f_+/f_- discussed in Sec. IV B below.

In each figure the solid line is the $u^{(1)}$ solution (arbitrarily normalized to unity at $p = 0$), the dashed line is the $u^{(2)}$ solution, and the dotted line is the sum $u^{(+)} = u^{(1)} + u^{(2)}$. Note that all of the wave functions have long "tails" which extend to several GeV, but that the sum $u^{(+)}$ falls off much more rapidly. Except for some structure at small momentum, $u^{(2)} \cong -u^{(1)}$, as suggested by the solution (4.5), and this relation holds to a better approximation as the pion mass μ decreases.

The values of $100 \times \mu^2$ (in GeV^2) and $1/p_0^2$ (in GeV^{-2}) are plotted as a function of the (small) parameter $\epsilon = 1 - 2\frac{C}{m_u}$ in Fig. 3. Note that the first few solutions satisfy the relation (the dashed line in the figure)

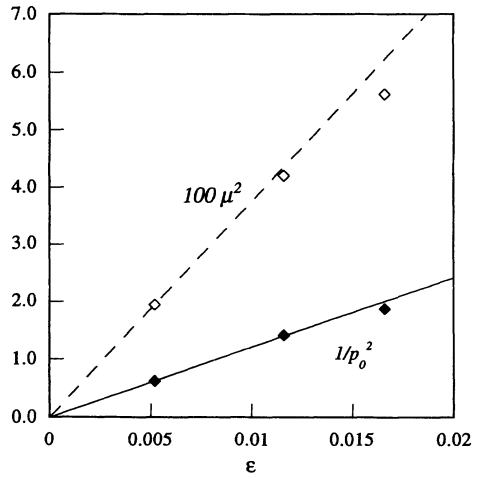

FIG. 3. The values of $100\mu^2$ (open diamonds) and $1/p_0^2$ (solid diamonds), in GeV units, plotted against the "eigenvalue" $\epsilon = 1 - 2\frac{C}{m_u}$ for the three solutions discussed in the text. The dashed line is Eq. (4.6) with $a_1 = 3.75$ and the solid line is Eq. (4.24) with $1/a_2 = 121.1$.

$$\mu^2 = a_1\left(1 - \frac{2C}{m_u}\right), \tag{4.6}$$

where $a_1 \cong 3.75$ GeV^2. When combined with Eq. (2.8) for the dynamical generation of quark mass, this leads to a Gell Mann, Oakes, and Renner relation [7]

$$\mu^2 = 4a_1\frac{m_0}{m_u}, \tag{4.7}$$

which gives a (renormalized) current quark mass of $m_0 \cong 1.7$ MeV, in qualitative agreement with current thinking.

B. Stability of the pion

In this section we will show how the constant and linear parts of the potential cooperate to produce a stable, low mass pion state, and that the relativistic nature of the equations is an essential aspect of the description. Our discussion is a generalization of Feynman's famous argument which uses the uncertainty principle to show that the hydrogen atom is stable [8].

In order to develop the argument we use the fact that the primary feature of the exact solution shown in Fig. 2 is the long, smooth "tail" which falls off slowly with momentum. The large solution $u^{(1)}$ also has a distinctive, rapidly varying low momentum structure. By comparing $u^{(1)} + u^{(2)}$ with the integral

$$I_{12} = \int V_{12}\, u^{(2)}\,, \tag{4.8}$$

both of which are shown in Fig. 2 for the $\mu = 0.1397$ solution, we conclude that this structure comes from the off-diagonal linear potential, and arises from the way in which we have removed the singularities of V_{12}. We will assume that this is not an "essential" feature of the solution, and that the average properties of the pion can be understood by ignoring this detail. In this case the two components of the pion wave function, $u^{(1)}$ and $u^{(2)}$, have essentially the same shape with an average momentum which is much larger than the quark mass.

In order to understand these solutions, it is convenient to consider the equations for the coupled amplitudes $u^{(\pm)}$ introduced in Eq. (4.1). These equations are

$$\begin{aligned} 2E_p\left(1 - \frac{2C}{m}\right)u^{(-)} - \mu\, u^{(+)} &= -\int \frac{d^3k}{(2\pi)^3} V_{--}\, u^{(-)} \\ &\quad - \int \frac{d^3k}{(2\pi)^3} V_{-+}\, u^{(+)}, \\ -\mu\, u^{(-)} + \left(2E_p + \frac{2Cm}{E_p}\right)u^{(+)} &= -\int \frac{d^3k}{(2\pi)^3} V_{+-}\, u^{(-)} \\ &\quad - \int \frac{d^3k}{(2\pi)^3} V_{++}\, u^{(+)}, \end{aligned} \tag{4.9}$$

where the potential kernels are

$$V_{\rho\rho'} = \frac{1}{2}\frac{(V_{11} + \rho\rho' V_{22})\,\mathbf{A} + (\rho' V_{12} + \rho V_{21})\,\mathbf{B}}{(1+\tilde{p}^2)(1+\tilde{k}^2)}\,, \tag{4.10}$$

with $\mathbf{A}$ and $\mathbf{B}$ defined in Eq. (3.12), and ρ and ρ' can both

be either + or −. If we then integrate these coupled equations for $u^{(\pm)}$ over the external momentum p, we are led to the following simple coupled equations for the mean values of the wave functions $f_\pm = \int dp\, u^{(\pm)} = \langle u^{(\pm)} \rangle$:

$$2E_0\left(1-\frac{2C}{m}\right)f_- - \mu f_+ = -\left\langle \int V_{--}u^{(-)} \right\rangle - \left\langle \int V_{-+}u^{(+)} \right\rangle,$$
$$-\mu f_- + \left(2E_0 + \frac{2Cm}{E_0}\right)f_+ = -\left\langle \int V_{+-}u^{(-)} \right\rangle - \left\langle \int V_{++}u^{(+)} \right\rangle, \tag{4.11}$$

where E_0 is the mean value of the energy E_p. If p_0 is the mean momentum, we will assume that, for any function F, $\langle F(p)\rangle \simeq F(p_0)$, so that $E_0 = \sqrt{m^2+p_0^2}$. The matrix elements of the linear potential have the form

$$\left\langle \int V_{\rho\rho'}u^{(\rho')} \right\rangle \simeq \int dp \int dk V_{\rho\rho'}(p,k)u^{(\rho')}(k)$$
$$\simeq \langle\langle V_{\rho\rho'}\rangle\rangle\, f_{\rho'}\ , \tag{4.12}$$

where the repeated ρ' indicies are not summed.

The next step in the argument is to express the mean values of the linear potential matrix elements in terms of p_0, μ, and $f_\pm$. To this end we note that

$$\tilde{A} = \frac{\mathbf{A}}{(1+\tilde{p}^2)(1+\tilde{k}^2)} = \frac{m^2+E_pE_k-pkz}{2E_pE_k},$$
$$\tilde{B} = \frac{\mathbf{B}}{(1+\tilde{p}^2)(1+\tilde{k}^2)} = \frac{m^2-E_pE_k-pkz}{2E_pE_k} = -1+\tilde{A}\ . \tag{4.13}$$

In the Appendix, we show that the integrals are dominated by values of these functions where p and k are much greater than the quark mass m, and where $p=k$ and $z=1$, so that, for the purposes of this simple estimate, we may approximate $\tilde{A}$ by

$$\tilde{A} \simeq \frac{m^2(p+k)^2}{(2pk)^2} \simeq \frac{m^2}{p^2}\ . \tag{4.14}$$

Using this expression we show in the Appendix that the moments of the potentials can be approximated by [recall Eq. (4.12)]:

$$\langle\langle V_{ij}\tilde{\theta}\rangle\rangle \simeq \frac{\sigma_{ij}}{p_0} - 2\lambda_{ij}\mu\ , \tag{4.15}$$

where $\tilde{\theta}$ is either $\tilde{A}$ or $\tilde{B}$, and the σ_{ij} and λ_{ij} are constants. It is a good approximation to take $\sigma_{11}=\sigma_{22}=\sigma_1$ and $\sigma_{12}=\sigma_{21}=\sigma_2$, and then the remaining constants can be expressed in terms of these two, and one other constant λ, as follows:

$$\lambda_{11} = \frac{1}{2}\sigma_1 b_{11}, \qquad \lambda_{12} = \frac{1}{2}\sigma_2 b_{21} - \lambda,$$
$$\lambda_{21} = \frac{1}{2}\sigma_2 b_{21}, \qquad \lambda_{22} = \frac{1}{2}\sigma_1 b_{22}\ , \tag{4.16}$$

where, if all units are in GeV,

$$b_{11} = 1.31, \qquad b_{22} = 1.66, \qquad b_{21} = 2.94\ . \tag{4.17}$$

The arguments leading to these estimates are presented in some detail in the Appendix, but will also be summarized here.

The σ/p_0 term in each expression is a direct consequence of the uncertainty principle, which implies that the mean momentum p_0 of a confined system is inversely proportional to its size $\langle r\rangle$ so that the average value of the linear confining term goes as $\sigma\langle r\rangle \simeq \sigma/p_0$. When the momentum is larger than the quark mass relativistic effects modify this simple result, but the modification is cancelled by the m^2/p^2 term in $\tilde{A}$ and $\tilde{B}$, so that the simple estimate is correct in both the nonrelativistic and ultrarelativistic limits. The kernels also depend explicitly on the pion mass through (i) the quark form factors, Eq. (3.20), (ii) the retardation factors in the off-diagonal kernels, Eq. (3.21), (iii) the limits of integration in the off-diagonal kernels, Eq. (3.16), and (iv) the "−1" term in $\tilde{B}$. The first three of these mass dependences can be combined into functions which multiply each of the "leading" σ/p_0 terms. These functions can be approximated by linear relations of the form $c_{ij}[1-b_{ij}p_0\mu]$, where the b_{ij}'s can be estimated [cf. Eq. (4.17)], and the constants c_{ij} (which are harder to estimate reliably) absorbed into the definition of the σ_i's. It turns out that $c_{11}=c_{22}>c_{12}=c_{21}$, which explains why $\sigma_{11}=\sigma_{22}=\sigma_1>\sigma_{12}=\sigma_{21}=\sigma_2$. Finally, the mass dependence associated with the "−1" term in $\tilde{B}$ could contribute to both of the off-diagonal kernels, but because of the condition Eq. (3.22) and the fact that the actual solutions are very close to $1/E$, this additional contribution to the V_{21} kernel is very small (and is taken to be zero). The size of the "−1" contribution to the V_{12} kernel is hard to estimate, but since it goes to zero as $\mu\to 0$, it is approximated by $2\lambda\mu$, with λ an unknown constant.

Using the estimates (4.15), the $V_{\rho\rho'}$ kernels are

$$\langle\langle V_{--}\rangle\rangle \simeq \frac{\sigma_1-\sigma_2}{p_0} - \lambda_{--}\mu, \qquad \langle\langle V_{-+}\rangle\rangle \simeq -\lambda_{-+}\mu,$$
$$\langle\langle V_{++}\rangle\rangle \simeq \frac{\sigma_1+\sigma_2}{p_0} - \lambda_{++}\mu, \qquad \langle\langle V_{+-}\rangle\rangle \simeq -\lambda_{+-}\mu\ , \tag{4.18}$$

where

$$\lambda_{\rho\rho'} = \lambda_{11} + \rho\rho'\lambda_{22} + \rho'\lambda_{12} + \rho\lambda_{21}\ . \tag{4.19}$$

Then Eqs. (4.11) become

$$2p_0\epsilon f_- - \mu f_+ = -\left(\frac{\sigma_1-\sigma_2}{p_0} - \lambda_{--}\mu\right) f_- + \lambda_{-+}\mu f_+ ,$$
$$-\mu f_- + \left(2p_0 + \frac{2m^2}{p_0}\right) f_+ = \lambda_{+-}\mu f_- - \left(\frac{\sigma_1+\sigma_2}{p_0} - \lambda_{++}\mu\right) f_+ , \tag{4.20}$$

where we have introduced $\epsilon = \left(1 - \frac{2C}{m}\right)$, have assumed that $p_0 >> m$, and kept terms up to order $1/p_0$ except for terms of order ϵ/p_0, which are neglected. We have studied the most general solutions of these equations, and found that the observed linear dependence of μ^2 on ϵ, Eq. (4.6), can be obtained only if $\lambda_{-+} \simeq -1$, so we simplify the discussion here by imposing the condition

$$\lambda_{-+} = -1 \tag{4.21}$$

from the start. In this case the small component f_+ drops out of the first equation, giving

$$\left[2p_0\,\epsilon + \frac{\sigma_1-\sigma_2}{p_0} - \lambda_{--}\mu\right] f_- = 0 . \tag{4.22}$$

Hence the pion mass, as a function of its mean internal momentum, p_0, is

$$\mu = \frac{1}{\lambda_{--}}\left[2p_0\,\epsilon + \frac{\sigma_1-\sigma_2}{p_0}\right] . \tag{4.23}$$

The correct mean momentum is the one for which the pion is stable, i.e., the value at which the pion mass is a minimum. This point occurs at

$$p_0^2 \simeq \frac{\sigma_1-\sigma_2}{2\epsilon} = \frac{a_2}{\epsilon} . \tag{4.24}$$

Substituting this into Eq. (4.23) and solving for μ^2 gives Eq. (4.6) with

$$a_1 = \frac{8\,(\sigma_1-\sigma_2)}{\lambda_{--}^2} . \tag{4.25}$$

The equations (4.6) [with a_1 given by (4.25)] and (4.24) explain the linear dependence of both μ^2 and $1/p_0^2$ on the quantity $1 - 2C/m$, as shown in Fig. 3. The straight line fits shown in Fig. 3 correspond to $a_1 = 3.75$ and $1/a_2 = 121.1$, which emerge if we take $\lambda_{--} = 0.1877$ and $\sigma_1 - \sigma_2 = 0.0165$ GeV^2. The values of p_0 for each case are shown in Table I; note that they are all comfortably larger that the quark mass, as assumed in the discussion.

The three equations (4.21), (4.24), and (4.25) fix the three parameters σ_1, σ_2, and λ. If all units are expressed in GeV, these are

$$\sigma_1 = 0.5282 , \qquad \sigma_2 = 0.5116 , \qquad \lambda = 0.8152 . \tag{4.26}$$

Now that the parameters are known, we may return to the coupled equations (4.20) and use our results to predict the ratio of f_+/f_-. From the second of the Eqs. (4.20) we obtain

$$\frac{f_+}{f_-} = \frac{\mu}{2p_0}\left[\frac{1+\lambda_{+-}}{1 + \dfrac{2m^2+\sigma_1+\sigma_2}{2p_0^2} - \dfrac{\lambda_{++}\mu}{2p_0}}\right] \simeq \frac{19.34\,\epsilon}{1+61.04\,\epsilon} . \tag{4.27}$$

This gives a result in fair agreement with the exact solutions, as shown in Table I and Fig. 4.

Using the values of the parameters we have determined, the matrix elements of the kernel are

$$\langle\langle V_{11}\tilde{A}\rangle\rangle \simeq \frac{0.5282}{p_0} - 0.6919\mu,$$
$$\langle\langle V_{22}\tilde{A}\rangle\rangle \simeq \frac{0.5282}{p_0} - 0.8768\mu,$$
$$\langle\langle V_{12}\tilde{B}\rangle\rangle \simeq \frac{0.5116}{p_0} + 0.1263\mu,$$
$$\langle\langle V_{21}\tilde{B}\rangle\rangle \simeq \frac{0.5116}{p_0} - 1.5041\mu , \tag{4.28}$$

where all quantities are in units of GeV.

Now that we have a qualitative description of the solutions, it is easier to discuss the physics contained in our model. First, in the chiral limit when $\mu \to 0$ and $\sigma_1 \to \sigma_2$, all of the kernels will approach σ/p_0 [where $\sigma = \frac{1}{2}(\sigma_1+\sigma_2)$]. Yet this limiting term plays practically no role in the final description of the pion, and it is not clear that we could even obtain a solution if the interaction contained *only* these terms. If the chiral symmetry breaking terms in the linear potential were ignored (i.e., if the $\sigma_1-\sigma_2$ terms and the μ-dependent terms in the off-diagonal potentials were all discarded), the determinant of the coupled equations (4.20) would give

$$\mu^2 = 4\epsilon\left(p_0^2 + m^2 + \sigma\right) . \tag{4.29}$$

This gives a pion mass which approaches zero as $\epsilon \to 0$ (with a linear dependence on ϵ), but the solution stabilizes at $p_0 = 0$, showing that the quarks are not confined. Thus a reasonable description of a physical pion of finite size cannot be obtained by using only the chiral limit of

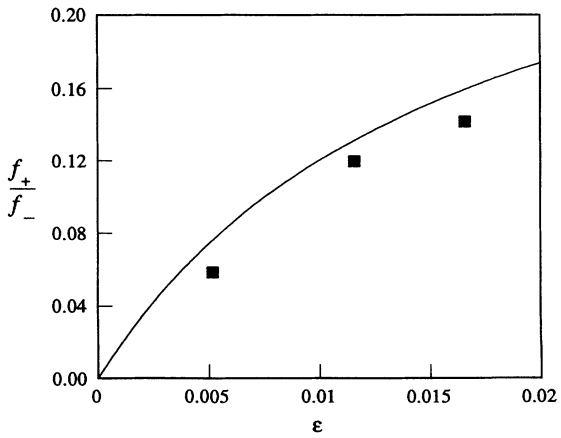

FIG. 4. The ratio f_+/f_- as a function of ϵ for the three solutions discussed in the text (solid squares). The solid line is the predicted result, Eq. (4.27).

TABLE II. Masses (in MeV) for the first few meson states.

	Light quark states $m_u = 325$			Heavy quark states $m_c = 1400$	
	Theory	Expt.		Theory	Expt.
π	139.7	139.6	η_c	3070	2979
$\pi(1300)$	1237	1300±100		3540	3590(?)
ρ/ω	785	768/782	J/Ψ	3071	3097
D	1173	$\omega(1390)$	$\Psi(2S)$	3540	3686
$2S$	1240	$\rho(1450)$	Ψ(D)	3656	3770

the confining interaction, which confirms our initial observation [1, 2] that those contributions from the linear potential which survive in the chiral limit will decouple from the description of the physical pion.

However, it is incorrect to conclude from these observations that the linear potential plays no role in determining the mass and size of the physical pion. In fact, both of these quantities are very sensitive to precisely how chiral symmetry is broken by the confining forces. For example, had we neglected the second channel (by setting $\sigma_2 = 0$ and neglecting all of the μ-dependent terms in the kernels), the determinant of the coupled equations would give

$$\mu^2 = 4p_0^2\epsilon + 2\sigma_1 + \left(2m^2 + \sigma_1\right)\left(2\epsilon + \frac{\sigma_1}{p_0^2}\right) . \quad (4.30)$$

This equation gives a pion with mass $\mu^2 = 2\sigma_1 \neq 0$ when $\epsilon \to 0$, and shows again that the second channel is needed to obtain the correct chiral limit. Of course a scalar linear potential does break chiral symmetry, but if the second channel is retained, we still recover the limit $\mu \to 0$ as $\epsilon \to 0$. The difference in strength of the diagonal and off-diagonal interactions, approximated by the constant $\sigma_1 - \sigma_2$, drives the mean momentum to infinity as $\epsilon \to 0$ [recall Eq. (4.24)], and the term dependent on $\lambda_{--}\mu$ ensures that μ^2 and $1/p_0^2$ are both linear in ϵ (at least for very small ϵ). These two terms ensure that the strength of the diagonal and off-diagonal potentials will be equal in the chiral limit by forcing them both to zero. The pion becomes a point particle, permitting us to regard it as a fundamental field, which is nicely consistent with (but not required by) its interpretation as a Goldstone boson. Finally, as discussed above, the condition (4.21) ensures that the linear dependence of μ^2 and $1/p_0^2$ on ϵ holds over a wide range of ϵ.

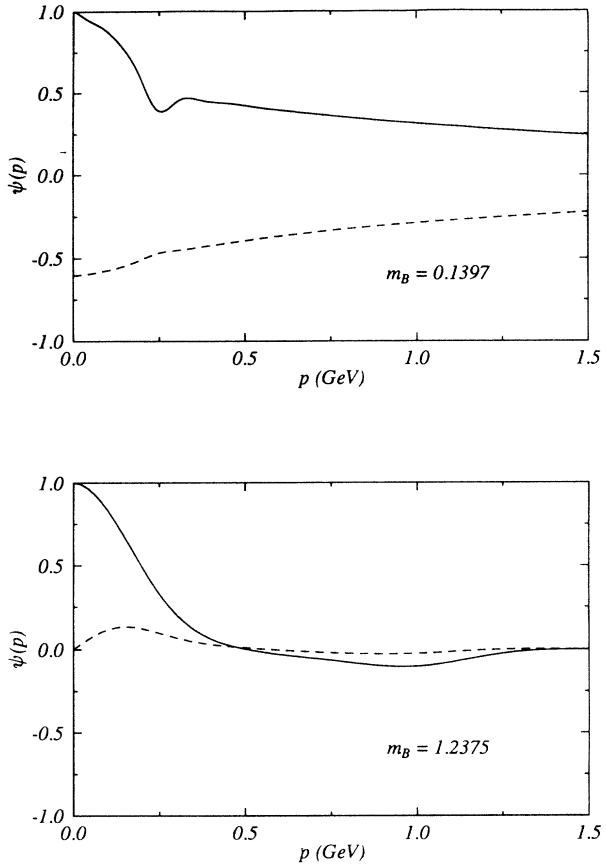

FIG. 5. Solutions for pion and its first excited state. In the top figure the solid line is $u^{(1)}$ and the dashed line is $u^{(2)}$. In the lower figure, the solid line is $u^{(1)}$ and the dashed line is $v^{(1)}$.

In conclusion, this model gives a pion with two highly relativistic constituents and with a structure sensitive to the detailed way in which the linear confining interaction breaks chiral symmetry. These points will be discussed further in Sec. VI.

V. NORMAL MESONS

We now turn to a discussion of how the model describes mesons other than the pion. For these mesons the mass m_B is comparable to the dynamical quark mass, and the mean momentum is related to the mass difference $m_B - 2m$, as in conventional quantum mechanics. Under these conditions it is a good approximation to neglect the coupling to channel 2, and the equations therefore become

$$\left[2E_p\left(1 - \frac{C}{m}\right) + C\frac{m}{E_p} - m_B\right]U(p) + C\frac{p}{E_p}\mathbf{a}V(p) = -\int \frac{d^3k}{(2\pi)^3}V_{11}\frac{\mathbf{A}U(k) + \mathbf{E}_+(p,k)V(k)}{(1+\tilde{p}^2)(1+\tilde{k}^2)},$$

$$C\frac{p}{E_p}\mathbf{a}^T U(p) - \left(C\frac{m}{E_p} + m_B\right)V(p) = -\int \frac{d^3k}{(2\pi)^3}V_{11}\frac{\mathbf{E}_+^T(k,p)U(k) - \mathbf{D}V(k)}{(1+\tilde{p}^2)(1+\tilde{k}^2)}, \quad (5.1)$$

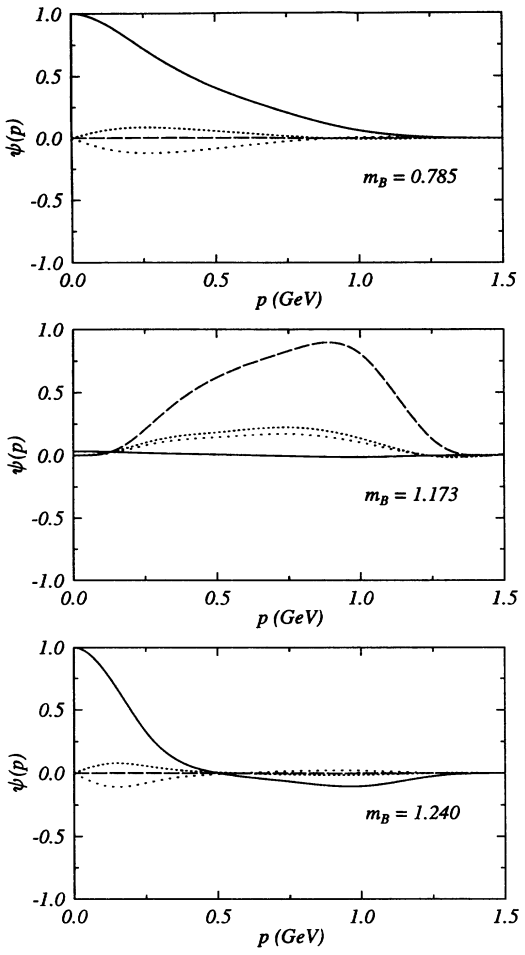

FIG. 6. Solutions for ρ and its first two excited states. In each figure the solid line is u, the dashed line is w, the closely spaced dotted line is v_s, and the widely spaced dotted line is v_t.

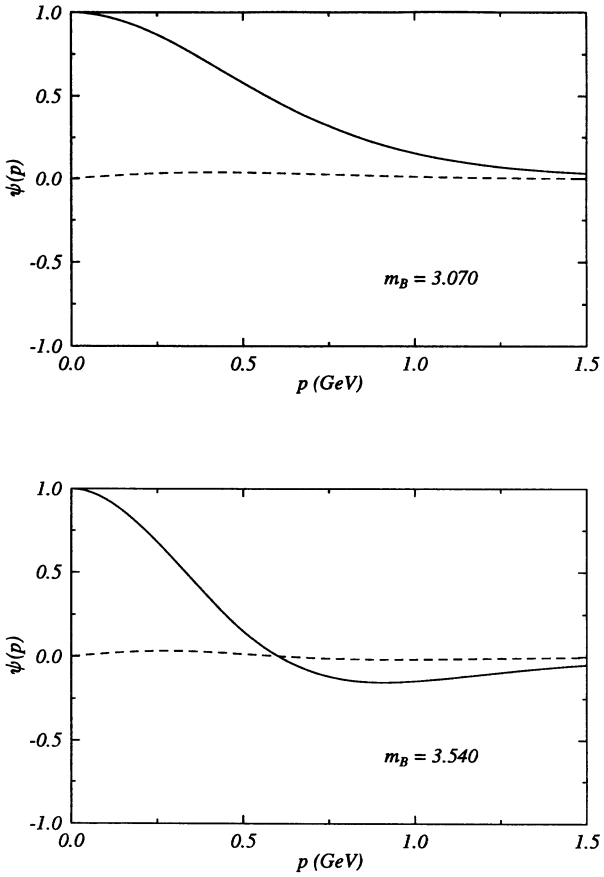

FIG. 7. Solutions for η_c and its first excited state. In each figure the solid line is u, the dashed line is v (channel 1).

where the quantities $\mathbf{a}$, $\mathbf{A}$, $\mathbf{D}$, and $\mathbf{E}_\pm$ were defined in Eqs. (3.10), (3.12), and (3.13). For the pseudoscalar states, $U(p) = u^{(1)}(p)$, $V(p) = v^{(1)}(p)$, $\mathbf{a} = 1$, and Eqs. (5.1) are two coupled equations for the S- and P-state components of the meson wave function. For vector states,

$$U(p) = \begin{pmatrix} u^{(1)}(p) \\ w^{(1)}(p) \end{pmatrix}, \qquad V(p) = \begin{pmatrix} v_s^{(1)}(p) \\ v_t^{(1)}(p) \end{pmatrix}, \tag{5.2}$$

as discussed in Sec. III. Now Eqs. (5.1) are four coupled equations for the S, D, and triplet and singlet P states.

The masses of the lowest lying pseudoscalar and vector states are listed in Table II, and wave functions are shown in Figs. 5–8. For completeness, the physical pion (with mass $m_B = 0.1397$ GeV) is also given in Table II and shown in Fig. 5. The additional parameters are the strength of the constant potential $C = 0.4974 \times 325 = 161.655$ MeV, the strength of the linear confining potential $\sigma = 0.2$ GeV^2, and the form factor masses $\Lambda = 1.7m$ and $\Lambda_q = 3.5m$, which scale with the quark mass. The dynamical mass for the light quark states is $m = m_u = 325$ MeV, and for the heavy quark states is $m = m_c = 1400$ MeV. Note that the first excited S state, labeled $2S$, lies above the D state in the light quark sector, but lies below the D state in the heavy quark sector.

We discuss these results and draw conclusions from this work in the following section.

VI. DISCUSSION AND SUMMARY OF THE RESULTS

In this work we have focused on the role of chiral symmetry and on the quantitative treatment of the chiral symmetry breaking terms which arises from the fact that the current quark mass is nonzero and the linear part of the confining interaction is presumably a scalar in Dirac space. Our work complements a number of other recent works which also treat mesons as relativistic bound states of the $q\bar{q}$ system. Some of these works also discuss the role of chiral symmetry [9–11], but in all of these works the confining interaction is chirally symmetric, and therefore cannot be taken to be a pure scalar. To our knowledge, this work is the first to show that a zero mass pion can emerge as the current quark mass approaches zero,

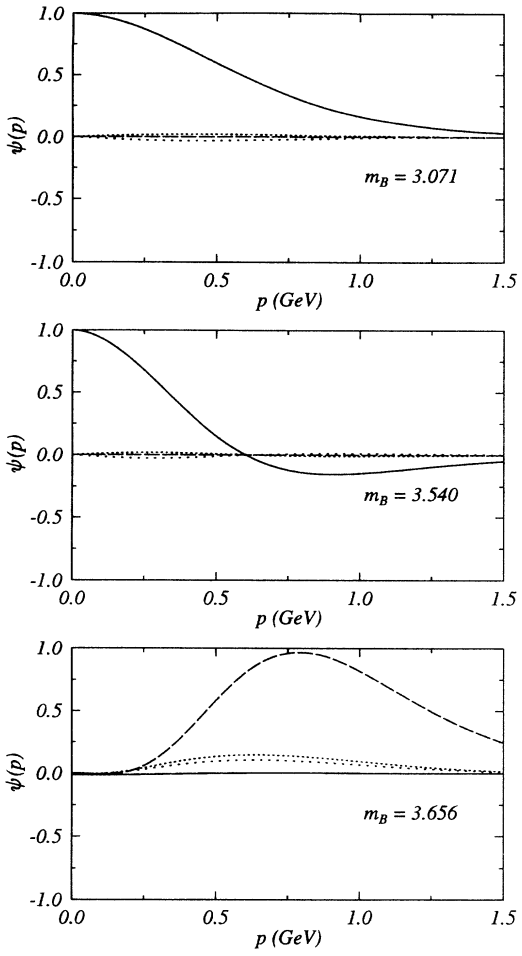

FIG. 8. Solutions for J/Ψ and its first two excited states. The curves in each figure are as in Fig. 6.

even though the confining interaction is a chirally violating scalar interaction. Other recent works do not discuss the role of chiral symmetry or the origin of the dynamical mass of the quarks [12, 13]. The most ambitious of these is the study by Tiemeijer and Tjon [12], who have succeeded in describing the meson spectrum and decays using relativistic two-body equations similar to (but different from) ours. Among the many things they find is that a global fit to meson excited states (the Regge trajectories) is greatly improved by allowing the linear confining interaction to be a mixture of about 80% scalar and 20% vector, and that even in this favorable case a good fit to the trajectories requires the total strength of the linear confining interaction to be at least $\sigma \simeq 0.33$ GeV^2, considerably larger than the strength $\sigma \simeq 0.2$ GeV^2 required by nonrelativistic equations and also contrary to the results suggested by lattice gauge calculations. Their work suggests that our model, when extended to higher excited states, may also require such an admixture, and may suffer from the same problem. Other studies using an instantaneous approximation have also found that a linear combination of vector and scalar confinement may be important [14, 15].

One unsatisfactory feature of our work is the appearance of form factors. It may be possible to eliminate the form factor which regulates the large q^2 behavior of the $1/q^4$ term in the kernel [the one which depends on Λ^2 in Eq. (3.18)] by using the method recently introduced by Hersbach and Ruijgrok [16]. In any case this form factor is used only to regulate the quark self-energy, which could be regulated is some other way. The quark form factor, given in Eq. (3.19), is sufficient to ensure the convergence of the bound state equations, but also affects the large momentum behavior of the excited solutions in the light quark sector, as shown in Figs. 5 and 6. Perhaps it can also be replaced using the method of Ref. [16], or by a more sophisticated treatment of the quark self-energy.

We close this section with a brief summary of the principal results of this paper:

(i) Using a relativistic model with the interaction kernel (1.1), which consists of only a *constant vector* plus a *linear scalar* interaction [with *no* one-gluon-exchange (OGE) term], we obtain Eq. (2.8) for the dynamical generation of quark mass. This equation relates the strength of the constant vector interaction C to the difference between the dynamical quark mass of the light quarks which make up the pion, m_u, and the current mass of these light quarks m_0: $C = (m_u - m_0)/2$. Using a dynamical quark mass of $m_u = 325$ MeV, we find a fit to the pion mass gives $C = 161.655$ MeV (where, because of the extreme sensitivity of the equations to the small parameter $\epsilon = 1 - \frac{2C}{m_u} = m_0/m_u$, C must be given to six significant figures if the pion mass is to be determined to four significant figures), and hence a current quark mass of $m_0 \simeq 1.7$ MeV, in qualitative agreement with current thinking.

(ii) In common with the NJL model, our relativistic equations (3.1) have the property that the pion mass automatically approaches zero in the chiral limit when $C \to m_u/2$ (or $m_0 \to 0$), *even though the linear part of the interaction is a scalar* and thus breaks chiral symmetry. This result is due to the constraint (1.3), which arises from the physical requirement that the linear interaction be zero when the two quarks occupy the same point in coordinate space. The decoupling of the linear confining interaction is, then, a consequence of the result that the pion is, in our approach, pointlike in the chiral limit.

(iii) Using four parameters which are the same for all sectors [the strengths of the constant interaction C and of the linear interaction $\sigma = 0.2$ GeV^2, and two form factor masses $\Lambda = 1.7m$ and $\Lambda_q = 3.5m$ which scale with the quark mass m] and the dynamical quark masses, which must be chosen for each sector, we are able to describe the gross features of the meson spectrum.

(iv) The light quark sector consisting of the pion (and its excited states) and the ρ and/or ω (and its excited states) is reasonably well explained by choosing $m_u = 325$ MeV [and $C = 161.655$ MeV as discussed above]. Note that, even though there is no OGE term, this choice of quark mass gives a good separation between the pion and the ρ and/or ω, and we also obtain a large splitting between the pion and its first excited state, in good agreement with experiment (see Table II). The first excited S and D states of the vector mesons are about

200 MeV too low. Experience with nonrelativistic models leads us to believe that addition of OGE should improve the splittings and contribute to the meson masses, but this model suggests that the smallness of the pion mass is due primarily to coupling to a second channel, required by chiral symmetry, and not to the OGE force. However, the constant part of the interaction we are proposing has a pure $\gamma^\mu\gamma_\mu$ vector structure, and hence might be regarded as arising ultimately from the renormalization of the OGE force.

(v) The choice of $m_c = 1400$ MeV gives a reasonable account of the low-lying charmonium spectrum, including the splitting between the η_c and the J/Ψ, but other splittings are $\sim$100 MeV too small, as might be expected for a model without the spin-spin interaction of a perturbative, OGE force.

Some of these results, the π-ρ mass splitting and the quark self-energy, will be modified once the full OGE force has been added to this model. However, one may view our constant interaction, which is purely vector, to be a first approximation to a full incorporation of a nonperturbative OGE force. In particular, the constant term may ultimately owe its origin to the renormalization of the OGE contributions to the quark self energy. In this case, the remaining finite part of the OGE force may have less of an effect on the meson spectrum than is the case in most models.

In conclusion, our model gives a good account of the gross features of the meson spectrum and provides a natural explanation for the small pion mass.

ACKNOWLEDGMENTS

F.G. thanks B. Keister for helpful advice on the numerical treatment of singular integrals. This work was partially supported by DOE Grant Nos. DE-FG05-88ER40435 and DOE-FG02-93ER40762.

APPENDIX A

1. Estimates for the confining kernels

In this section we derive simple estimates for the linear confining kernels. These estimates are used in our discussion of the stability of the pion given in Sec. IV B.

A typical integral to be estimated is the V_{11} matrix element

$$\int V_{11}\tilde{A}\,u^{(1)} = \int \frac{d^3k}{(2\pi)^3}\frac{V_{11}(p,k)\mathbf{A}(p,k,z)}{(1+\tilde{p}^2)(1+\tilde{k}^2)}u^{(1)}(k)$$
$$= \int_0^\infty \frac{k^2dk}{(2\pi)^2}\int_{-1}^1 dz V_A(p^{(1)},k^{(1)})\left\{\tilde{A}(p,k,z)u^{(1)}(k) - \frac{E_p}{E_k}\tilde{A}(p,p,1)u^{(1)}(p)\right\}. \quad \text{(A1)}$$

For a first estimate we neglect both form factors, so that $V_A = -8\pi\sigma/q^4$, and exploit the fact that the z integral is dominated by the region near $z = 1$, where the integrand peaks. Then the z integral becomes, approximately,

$$\int_{-1}^1 dz V_A(p^{(1)},k^{(1)})\,\tilde{A}(p,k,z)u^{(1)}(k) \simeq \tilde{A}(p,k,1)\,u^{(1)}(k)\int_{-1}^1 dz V_A(p^{(1)},k^{(1)})$$
$$\simeq \frac{4\pi\sigma\tilde{A}(p,k,1)\,u^{(1)}(k)}{2pk\,[m^2 - E_pE_k + pk]}, \quad \text{(A2)}$$

where the term proportional to $1/[(E_p - E_k)^2 - (p+k)^2]$ was neglected. Inserting the estimate (A2) into (A1) gives

$$\int V_{11}\tilde{A}\,u^{(1)} \simeq \frac{\sigma}{2\pi}\int_0^\infty \frac{kdk\,\left[E_k\tilde{A}(p,k,1)\,u^{(1)}(k) - E_p\tilde{A}(p,p,1)u^{(1)}(p)\right]}{pE_k\,[m^2 - E_pE_k + pk]}. \quad \text{(A3)}$$

The denominator has a double zero at $p = k$, but the zero of the numerator at the same point ensures that the integral exists as a principle value, as in the nonrelativistic case. The behavior of the integrand depends on the behavior of the wave function $u^{(1)}$. Since $\tilde{A}(p,k,1)$ decreases monotonically in k, if $E_ku^{(1)}(k)$ does not increase then the integrand is positive for $k < p$ and negative for $k > p$, with a principal value singularity at $p = k$, as shown in Fig. 9. Hence the integral over a region from $k = 0$ to $k = k_0 \gg p$ is zero, and the entire result comes from values of $k > k_0$. If $E_k\tilde{A}(p,k,1)u^{(1)}(k)$ decreases sufficiently rapidly, the integral can therefore be approximated by

$$\int V_{11}\tilde{A}\,u^{(1)} \simeq -\left(\frac{\sigma}{2\pi}\right)\left(\frac{E_p}{p}\right)\tilde{A}(p,p,1)\,u^{(1)}(p) \times\int_{k_0}^\infty \frac{kdk}{E_k\,[m^2 - E_pE_k + pk]}. \quad \text{(A4)}$$

The remaining integral in Eq. (A4) diverges logarithmically, and will be cutoff by the form factors we have neglected so far in this discussion. If $p \ll m$, and assuming $\int dk/k \sim N_1$, the integral becomes

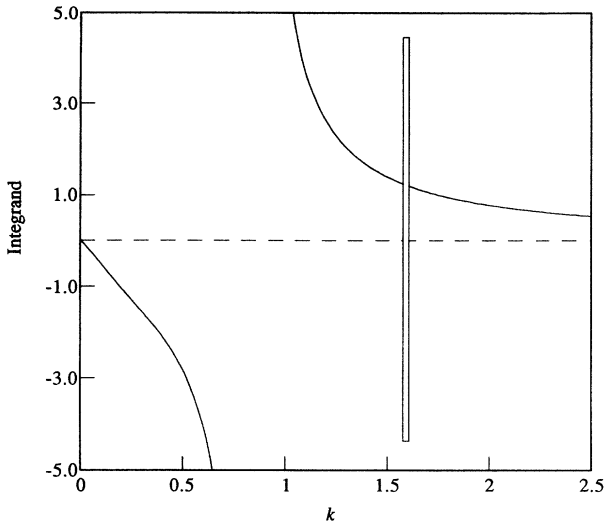

FIG. 9. The integrand of Eq. (A3) as a function of the internal momentum k for a fixed external momentum $p = 0.84$ GeV and a wave function proportional to $1/E$. The thin open box is in the vicinity of the point k_0; the region below k_0 makes no contribution to the integral.

$$\int_{k_0}^{\infty} \frac{kdk}{E_k\,[m^2 - E_pE_k + pk]} \simeq -\frac{2}{m}\int_{k_0}^{\infty} \frac{kdk}{(p-k)^2} \sim -\frac{2N_1}{m}\,. \tag{A5}$$

If $p \gg m$, the same integral becomes

$$\int_{k_0}^{\infty} \frac{kdk}{E_k\,[m^2 - E_pE_k + pk]} \simeq -\frac{2p}{m^2}\int_{k_0}^{\infty} \frac{kdk}{(p-k)^2} \sim -\frac{2pN_1}{m^2}\,. \tag{A6}$$

However [recalling Eq. (4.13)],

$$\tilde{A}(p,p,1) \simeq \begin{cases} 1, & \text{if } p \ll m, \\ \frac{m^2}{p^2}, & \text{if } p \gg m\,, \end{cases} \tag{A7}$$

and hence, in both limits [either $p \ll m$ or $p \gg m$],

$$\left(\frac{E_p}{p}\right)\tilde{A}(p,p,1)\int_{k_0}^{\infty} \frac{kdk}{E_k\,[m^2 - E_pE_k + pk]} \sim -\frac{2N_1}{p}\,, \tag{A8}$$

and

$$\left\langle\left\langle \int V_{11}\tilde{A} \right\rangle\right\rangle \simeq \frac{\sigma N_1}{\pi p_0} = \frac{\sigma_1}{p_0}\,, \tag{A9}$$

where our fits to the actual solutions give $N_1 \sim 2\pi$. Hence, in both the ultrarelativistic and nonrelativistic limits, the linear confining interaction contains a term which goes like $1/p_0$, as suggested by the uncertainty principle.

The kernels also depend explicitly on the bound-state mass μ. The diagonal terms depend on μ only through the quark form factors given in Eq. (3.20). Assuming that $p \gg m$, the form factors in both channels (1 and 2) are approximately equal, and a function of $(p\mu)^2$. Their precise dependence on the pion mass μ for a *fixed* momentum $p_0 = 0.84$ (corresponding to the mean momentum of the "middle" state at $\mu = 0.205$) and for the form factor mass used in this paper ($\Lambda_q = 3.5m$) is shown in Fig. 10. Note that they are approximately a linear function of μ in the vicinity of $\mu = 0.14 \to 0.25$, and if we require the intercepts of the two lines to be the same (in order to simplify the theoretical analysis) the form factors in each channel are well approximated by

$$\begin{aligned} f_1(\mu) &= f(m^2 + \mu^2 - 2E_0\mu) \simeq 1.12[1 - b_{11}\,p_0\mu], \\ f_2(\mu) &= f(m^2 + \mu^2 + 2E_0\mu) \simeq 1.12[1 - b_{22}\,p_0\mu]\,, \end{aligned} \tag{A10}$$

where the fits shown in Fig. 10 correspond to $b_{11} = 1.31$ and $b_{22} = 1.66$, the numbers used in Sec. IV B. These form factors modify both the p and k dependence of the kernels, but, as we will see below, the k integration is regularized more strongly by the smaller mass $\Lambda = 1.7m$, which provides convergence even when $\mu = 0$. Hence the μ dependence of the diagonal kernels comes primarily from the external p dependence, and we have finally

$$\begin{aligned} \left\langle\left\langle \int V_{11}\tilde{A} \right\rangle\right\rangle &\simeq \frac{\sigma_1}{p_0} - 2\lambda_{11}\mu, \\ \left\langle\left\langle \int V_{22}\tilde{A} \right\rangle\right\rangle &\simeq \frac{\sigma_1}{p_0} - 2\lambda_{22}\mu\,, \end{aligned} \tag{A11}$$

with $\lambda_{11} = \sigma_1 b_{11}/2$ and $\lambda_{22} = \sigma_1 b_{22}/2$.

The off-diagonal kernels have a more complex μ dependence coming from the external form factors, the retardation factor, and the μ dependence of the limits of integration. As discussed in some detail in our first paper [1], the V_{21} integrand has singularities over the region from k_- to k_+ [where $k_\pm$ were defined in Eq. (3.16)], and our prescription for the definition of the linear potential requires that this region be removed from the integration. Under the same assumptions used above, the remaining integrand is finite and negative in the region $[0, k_-]$, and finite and positive in $[k_+, \infty)$. For values of p in the vicinity of a GeV, $\int V_{21}\tilde{B}u^{(1)}$ can therefore be approximated (roughly) by

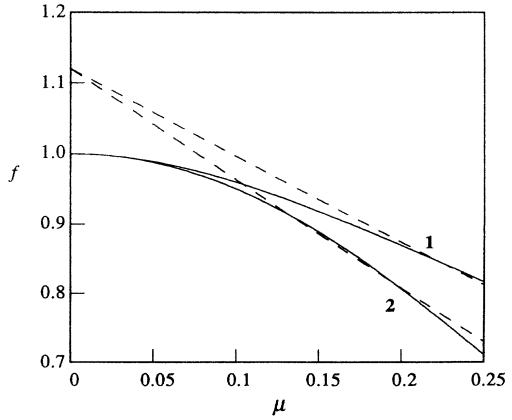

FIG. 10. The quark form factors Eq. (3.21) for channel 1 and 2 (labeled on the figure) plotted as a function of μ (in GeV) for a fixed $p = 0.84$ GeV. The straight line fits are Eqs. (A10).

$$\int V_{21}\tilde{B}\,u^{(1)} \simeq \frac{\sigma}{2\pi}\int_{k_++k_-}^{\infty} \frac{kdk\left[E_k\tilde{B}(p,k,1)\,u^{(1)}(k) - E_{k_+}\tilde{B}(p,k_+,1)u^{(1)}(k_+)\right]}{pE_k\left[m^2 - E_pE_k + pk + \mu(E_p - E_k) + \frac{1}{2}\mu^2\right]} . \tag{A12}$$

The numerator and denominator both have simple zeros at $k = k_+$, ensuring that the integrand is finite at $k = k_+$, so that the contribution from the region $[0, k_-]$ can be roughly included by adding k_- to the lower limit of integration [as in Eq. (A12)]. It turns out that the solutions are very close to $1/E$ over the momentum region of interest, so that we may replace $\tilde{B} = -1 + \tilde{A} \simeq \tilde{A}$, and if $p \gg m$, then $k_+ \simeq p$, and we obtain roughly

$$\begin{aligned}\int V_{21}\tilde{B}\,u^{(1)} &\simeq -\frac{\sigma}{2\pi}\,u^{(1)}(p)\,\tilde{A}(p,p,1)\int_{k_++k_-}^{\infty}\frac{kdk}{E_k\left[m^2 - E_pE_k + pk + \mu(E_p - E_k)\right]} \\ &\simeq \frac{\sigma}{2\pi}\,u^{(1)}(p)\,\frac{m^2}{p^2}\int_{k_++k_-}^{\infty}\frac{2pkdk}{m^2\left[(k-p)^2 + \dfrac{2\mu pk(k-p)}{m^2}\right]} ,\end{aligned} \tag{A13}$$

where we have retained the exact structure of the lower limit because the integral is sensitive to it. The integral is cutoff at large k by the mass Λ, which becomes effective when

$$-q^2 \sim 2[E_pE_k - m^2 - pk] \sim \frac{m^2(k-p)^2}{kp} \sim \Lambda^2 = (1.7m)^2 = 2.89m^2 . \tag{A14}$$

Finally, assuming $k \gg p$, as we did before, we obtain the following estimate

$$\begin{aligned}\left\langle\left\langle\int V_{21}\tilde{B}\right\rangle\right\rangle &\simeq \frac{\sigma}{\pi p_0}\frac{f_2(\mu)}{\left[1 + \dfrac{2\mu p_0}{m^2}\right]}\int_{k_++k_-}^{2.89p_0}\frac{dk}{k} \\ &\simeq \frac{\sigma}{\pi p_0}\frac{f_2(\mu)}{\left[1 + \dfrac{2\mu p_0}{m^2}\right]}\log\left(\frac{2.89}{\left[2 - \frac{\mu(2E_0+\mu)}{2p_0(E_0-p_0+\mu)} + \frac{\mu(2E_0+\mu)}{2p_0(E_0+p_0+\mu)}\right]}\right) \\ &\simeq \frac{\sigma N_2}{p_0}\,g_2(\mu) .\end{aligned} \tag{A15}$$

The functions $g_2(\mu)$ and $g_1(\mu)$ [obtained from g_2 by substituting $f_1(\mu)$ for $f_2(\mu)$], for the fixed momentum $p_0 = 0.84$ GeV, are shown in Fig. 11. They have been normalized to unity at $\mu = 0$; the unknown constant N_2 contains all normalization factors. Note that they can also be fit by a linear function of μ (assumed to scale as the product $p_0\mu$). The fits shown in Fig. 11 are

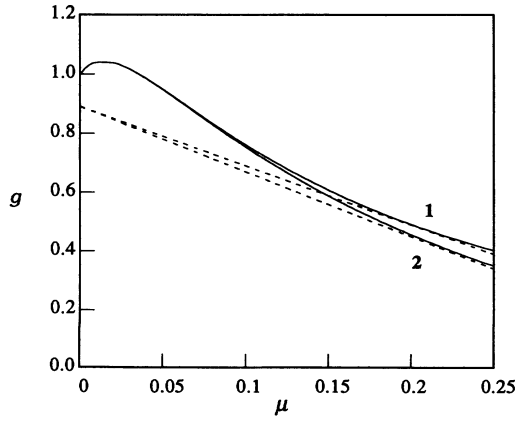

FIG. 11. The functions g_1 and g_2 (labeled 1 and 2 on the graph) plotted as a function of μ (in GeV) for a fixed $p = 0.84$ GeV. The straight line fits are Eqs. (A16).

$$\begin{aligned} g_1(\mu) &\simeq 0.89[1 - b'_{21}\,p_0\mu] , \\ g_2(\mu) &\simeq 0.89[1 - b_{21}\,p_0\mu] , \end{aligned} \tag{A16}$$

where $b'_{21} = 2.68$ and $b_{21} = 2.94$. The second of these curves is the correct one to use for the V_{21} kernel we have been discussing.

We turn now to the V_{12} kernel. Because of the symmetry of the matrix kernel, the V_{12} matrix element which we need can be obtained from the V_{21} matrix element with the k and p integrations interchanged. In particular

$$\left\langle\int V_{12}\tilde{B}\,u^{(1)}\right\rangle = \int d^3p\int d^3k\,u^{(1)}(p)\,V_{21}(p,k)\,\tilde{B}\,\frac{1}{4\pi k^2} . \tag{A17}$$

Recalling that $\tilde{B} = \tilde{A} - 1$, and carrying through the estimate as we did above, gives two terms. The $\tilde{A}$ term is identical to the result we have already obtained, but the contribution from the -1 term is no longer small. We know that it must go to zero as $\mu \to 0$, and can therefore be written as $2\lambda\mu$, with λ an undetermined constant. Our estimates of the off-diagonal potentials have therefore given

$$\left\langle\left\langle \int V_{12}\tilde{B} \right\rangle\right\rangle \simeq \frac{\sigma_2}{p_0} - 2\lambda_{12}\mu,$$
$$\left\langle\left\langle \int V_{21}\tilde{B} \right\rangle\right\rangle \simeq \frac{\sigma_2}{p_0} - 2\lambda_{21}\mu\,, \qquad \text{(A18)}$$

with $\lambda_{12} = \sigma_2 b_{21}/2 - \lambda$ and $\lambda_{21} = \sigma_2 b_{21}/2$. The constants σ_1, σ_2, and λ are adjusted to fit the results, as discussed in Sec. IV.

2. Numerical methods

In this section we discuss our numerical methods. The techniques are essentially extensions of those already discussed in our earlier papers [1, 2].

For a given bound-state equation, each wave function is expanded in terms of a set of basis functions $\{\beta_i(p)\}$:

$$\psi_i(p) = \sum_{j=1}^{n} \alpha_{ij}\beta_j(p). \qquad \text{(A19)}$$

The bound-state equation is then converted into a generalized eigenvalue problem, $A\mathbf{x} = \lambda B\mathbf{x}$, by integrating the entire equation over all momentum p using an appropriately chosen measure so that the matrix arising from the linear potential (and hence the entire matrix equation itself) is symmetric [recall that our potentials are Hermitian, $V_{ij}(p,k;P) = V_{ji}(k,p;P)$]. This last feature is particularly advantageous as it avoided the generation of spurious complex solutions due to round-off errors.

For the basis functions we used cubic B splines. While in our previous works we used other choices (Laguerre polynomials in Ref. [1]; generalized Yukawas, i.e., $(p^2 + M_i^2)^{n_i}$ in Ref. [2]), we found that they were not sufficiently flexible in the present case to solve the pion equation for arbitrary potential parameters. The difficulty here lay in matching the high momentum tail in our solutions, arising from the chiral-symmetry of our equations with the low momentum structure due to the scalar, linear potential. The advantage of B splines in this regard is that they naturally span large momentum scales while building in only minimal biases.

Although expansion in B splines is a well-known numerical technique, for the sake of completeness we give their definition and discuss some delicacies that were involved in their application to our equations. The cubic B splines are defined [17] so as to have finite support and to have a continuous first and second derivative. These requirements are achieved by piecing together four cubic polynomials, each defined only over a finite region. The points where the polynomials join are called knots. The cubic B spline $b_n(x)$, centered at knot x_n with equal spacing h between knots, is defined as [17]

$$b_n(x) = \frac{1}{4}\begin{cases} \left(\dfrac{x - x_{n-2}}{h}\right)^3, & x \in [x_{n-2}, x_{n-1}], \\ 1 + 3\dfrac{x - x_{n-1}}{h} + 3\left(\dfrac{x - x_{n-1}}{h}\right)^2 - 3\left(\dfrac{x - x_{n-1}}{h}\right)^3, & x \in [x_{n-1}, x_n], \\ 1 + 3\dfrac{x_{n+1} - x}{h} + 3\left(\dfrac{x_{n+1} - x}{h}\right)^2 - 3\left(\dfrac{x_{n+1} - x}{h}\right)^3, & x \in [x_n, x_{n+1}], \\ \left(\dfrac{x_{n+2} - x}{h}\right)^3, & x \in [x_{n+1}, x_{n+2}], \\ 0, & \text{otherwise.} \end{cases} \qquad \text{(A20)}$$

To obtain our basis functions $\{\beta_i(p)\}$, we start with n equally spaced B splines defined over the range $0 \le x \le 1$. For the pion case we then introduced a nonlinear (quadratic) mapping from x to momentum space in order to be adequately sensitive to the structure in both the low and high momentum regions. For all other cases, a simple linear mapping was sufficient (a high momentum cutoff $p_{\max}$ was introduced beyond which the wave functions were taken to be zero; after obtaining a solution, we then varied $p_{\max}$ to ensure that the solution was insensitive to its value). Each wave function was expanded with a basis set taken with the appropriate boundary condition at $p = 0$. As illustration, the complete set of S-wave basis functions in x space (normalized to one at the peak) for the case that $n = 4$ are shown in Fig. 12. Note that the derivative has been guaranteed to be zero at the origin. For the B spline with center at the origin, this is automatic. To the spline centered at $x = h$ was added the tail from the spline centered at $x = -h$. The basis set for P- and D-wave solutions were generated by multiplying the S-wave basis by p/E_p and $(p/E_P)^2$, respectively.

The presence of knots required special care in our integrations. All integrals were subdivided into pieces defined by the knots of the basis functions entering the integrand. Gaussian quadrature was then used to evaluate the integral of each subdivision. This procedure of

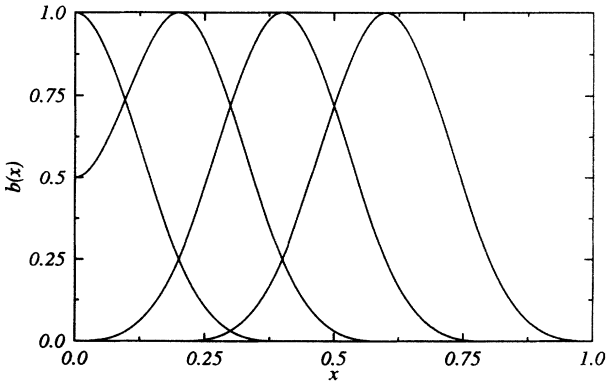

FIG. 12. The full set of cubic B splines used for S-wave solutions in the case $n = 4$. The derivative at the origin is zero by construction.

avoiding integration through the knots was essential, for without subdividing as many as twelve places of numerical accuracy could be lost (as, e.g., in the simple integral over two basis functions). Due to this necessity, the double integrals for the linear-potential matrix elements became rather complicated since in addition to the knots, the pole positions of the various potentials had to be specially handled. In the case of the diagonal potentials, V_{11}, V_{22}, which have single poles (after the subtraction) at $p = k$, symmetric integration in the k integral about the pole position was used in those cases where the matrix elements involved integrands with overlapping basis functions. For the case of the off-diagonal potentials, the region cutout of the integral in V_{21} [defined by the poles $k_1(p)$ and $k_2(p)$] introduced new integration limits that had to be properly incorporated (the V_{12} matrix elements were obtained using Hermiticity). Although in this case no pole remains in the potential after the subtraction, in order to ensure that the off-diagonal potentials smoothly matched onto the diagonal potentials in the limit that the pion mass went to zero, we integrated evenly below and above the pole positions k_1 and k_2.

In practice we solved our generalized eigenvalue problem for the bound-state mass after having chosen values for our parameters in the quark-quark interaction potential. Since the bound-state mass not only appears linearly in our equations in the kinetic terms, but also nonlinearly as part of the definition of the form factors of the linear potential, we used an iterative procedure of first guessing a value for the bound-state mass to be inserted into the confining potentials, then solving the eigenvalue problem and seeking a self-consistent solution. For all solutions other than the pion, the convergence of this procedure was rapid, as the dependence in the linear potential is very mild for large values of the bound state mass (i.e., for $\mu \approx 2m$). The pion, on the other hand, required more care. Finally, the number of basis functions were increased to check the convergence of our solutions. Except for the pion, this was also in general rapid ($n = 6$). The pion however, required significantly more ($n = 16$). The curves in Sec. IV were obtained using $n = 40$.

[1] F. Gross and J. Milana, Phys. Rev. D **43**, 2401 (1991).

[2] F. Gross and J. Milana, Phys. Rev. D **45**, 969 (1992).

[3] Y. Nambu and G. Jona-Lasinio, Phys. Rev. **122**, 345 (1961); **124**, 246 (1961).

[4] See L. S. Celenza, C. M. Shakin, W-D. Sun, J. Szweda, and X. Zhu, Brooklyn College Report No. BCCNT 93/031/230 (unpublished), for further discussion of confinement in the context of this approach.

[5] C. Michael, Phys. Rev. Lett. **56**, 1219 (1986); M. Campostrini, K. Moriarty, and C. Rebbi, *ibid.* **57**, 44 (1986); A. Huntley and C. Michael, Nucl. Phys. **B286**, 211 (1987).

[6] S. Godfrey and N. Isgur, Phys. Rev. D **32**, 189 (1985).

[7] M. Gell Mann, R. J. Oakes, and B. Renner, Phys. Rev. **175**, 2195 (1968); S. L. Adler and A. C. Davis, Nucl. Phys. **B244**, 469 (1984).

[8] R. P. Feynman, R. B. Leighton, and M. Sands, *The Feynman Lectures on Physics* (Addison-Wesley, Reading, MA, 1965), Vol. III, pp. 2–5.

[9] R. Horvat, D. Kekez, D. Palle, and D. Klabucar, "Covariant model of a quarkonium with the funnel potential," Zagreb University Report No. ZTF-93/9-R (unpublished); Phys. Rev. D **44**, 1585 (1991).

[10] P. J. A. Bicudo *et al.*, Phys. Rev. D **45**, 1673 (1992).

[11] P. Jain and H. J. Munczek, Phys. Rev. D **48**, 5403 (1993).

[12] P. C. Tiemeijer and J. A. Tjon, Phys. Rev. C **42**, 599 (1990); Phys. Lett. B **277**, 38 (1992); *ibid.* **48**, 896 (1993); P. C. Tiemeijer, Ph.D. thesis, University of Utrecht, 1993.

[13] A. Szczepaniak and A. G. Williams, Phys. Rev. D **47**, 1175 (1993).

[14] A. Archvadze, M. Chachkhunashvili, and T. Kopaleishvili, Few-Body Systems (to be published).

[15] C. R. Münz, J. Resag, B. C. Metsch, and H. R. Petry, Bonn Report Nos. TK-93-13 and TK-93-14 (unpublished).

[16] H. Hersbach and Th. W. Ruijgrok, Z. Phys. D **18**, 209 (1991); H. Hersbach, Phys. Rev. A **46**, 3657 (1992); Phys. Rev. D **47**, 3027 (1993); Ph.D. thesis, University of Utrecht, 1993.

[17] P. M. Prenter, *Splines and Variational Methods* (Wiley, New York, 1975).

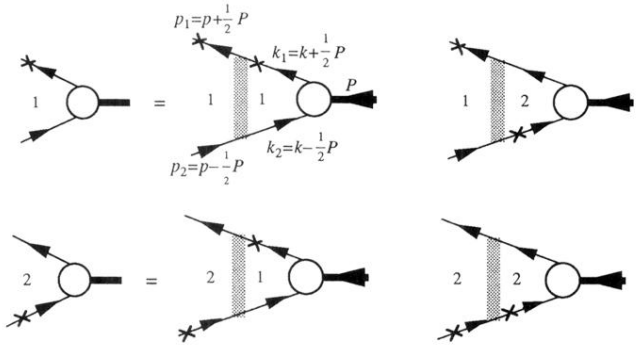

FIG. 1. Diagrammatic representation of the coupled channel bound state equations with the momenta and channel numbers labeled. The particle which is on shell is marked with an $\times$, and for channel 1 it is the quark and for channel 2 the antiquark. The wide shaded line connecting the two quarks represents the interaction kernel, which is a sum of constant plus linear terms.